Fuzzifying Images using Fuzzy Wavelet Denoising

Giovanni Palma, Isabelle Bloch, Serge Muller and Răzvan Iordache

***Abstract*— Fuzzy connected filters were recently introduced as an extension of connected filters within the fuzzy set framework. They rely on the representation of the image gray levels by fuzzy quantities, which are suitable to represent imprecision usually contained in images. No robust construction method of these fuzzy images has been introduced so far. In this paper we propose a generic method to fuzzify a crisp image in order to explicitly take imprecision on grey levels into account. This method is based on the conversion of statistical noise present in an image, which cannot be directly represented by fuzzy sets, into a denoising imprecision. The detectability of constant gray level structures in these fuzzy images is also discussed.**

I. Introduction

Connected filters are widely used in image processing. For instance detection or segmentation of structures can be achieved using the notion of flat zones [1]. Other kinds of filters exist like thinnings [2] that can help for the same task. These approaches rely on the extraction of connected components from a gray scale image according to a criterion on the gray levels within the input image. Thus, for flat zone oriented filters, connected components must have a constant gray level in the original image, while for thinnings component pixels must have gray levels less or equal to a given threshold.

Unfortunately, the behavior of these filters may be degraded when the input image is noisy or suffers from artifacts due to its acquisition. In order to overcome these issues, connected filters were recently extended into the fuzzy set theory [3]. In this new framework, image intensities are represented by fuzzy quantities leading to a fuzzy set defined on the image domain for each gray level. Fuzzy connected components are then extracted from these sets and filtered. Obviously, the construction of such images is a key point and has unfortunately not been conclusively investigated so far. In this paper we propose a generic solution to address this problem.

First, the context of fuzzy image filtering will be reminded. Then, a new fuzzification scheme based on wavelet decomposition is proposed. Finally, experiments illustrating the ability of the new method to detect structures in noisy images are commented.

II. The fuzzy image framework

Fuzzy images are able to represent imprecision on gray levels. In the most generic way, they are images whose intensities are represented by fuzzy quantities. In this section, we introduce these images and their filtering and we propose principles that allow constructing them.

A. Mathematical introduction to fuzzy images

Fuzzy images can mathematically be seen as fuzzy sets defined on $\Omega \times \mathcal{G}$ with Ω the image domain and $\mathcal{G}$ the set of gray levels. The set of these fuzzy images is denoted by $\mathcal{F}$ and for a fuzzy image $F \in \mathcal{F}$, a pixel $p \in \Omega$ and a gray level $g \in \mathcal{G}$, $F(p, g)$ represents the membership degree of some equality/inequality about g at point p according to the nature of F. The fuzzy quantity associated to a pixel of such a fuzzy image is denoted by $F(p, .)$. Additionally the spatial fuzzy set associated to a gray level is written $F(., g) \in \mathcal{S}$ with $\mathcal{S}$ the set of fuzzy sets defined on Ω. Adding properties to the fuzzy quantities associated to each pixel may lead to changes in the meaning of these images and of course to changes in the properties of filters that can be defined on them. Two major kinds of fuzzy images have been introduced so far.

The first one corresponds to fuzzy umbra images. The pixels of these images are represented by fuzzy quantities decreasing with respect to the gray level [3]:

Definition 2.1: A fuzzy image $F \in \mathcal{F}$ is a fuzzy umbra image (FUI) if:

$$\forall p \in \Omega, \forall (g_1, g_2) \in \mathcal{G}^2 \quad g_1 \leq g_2 \Rightarrow F(p, g_1) \geq F(p, g_2)$$

These images are fuzzy extensions of regular binary umbra images. The semantics of a FUI F is the following: for a given pixel p and a given gray level g, $F(p, g)$ represents the degree to which the image is greater or equal to g at point p.

In the second type of fuzzy images, pixel values are fuzzy numbers [4]:

Definition 2.2: A fuzzy image $F \in \mathcal{F}$ is a fuzzy number image (FNI) if:

$$\forall p \in \Omega \quad F(p, .) \textit{ is a fuzzy number}$$

Here the semantics for $F(p, g)$, with p a given pixel and g a given gray level, is the degree for the represented image to have the gray value g at pixel p.

The definitions of these fuzzy images, illustrated in Figure 1(a) and 1(b), are suitable to understand what they represent, but they unfortunately do not explain how to build them. Actually, they can be built in several ways. First, we can try to fuzzify the gray levels of a crisp image by applying a template on the gray levels as explained in [4]. Such a method is most of the time not suitable because images usually contain noise, which cannot be modeled correctly this way. Secondly, the imprecision of the acquisition system can be modeled in order to deduce the imprecision present

Serge Muller and Răzvan Iordache are with GE Healthcare, 283, rue de la Minière, 78530 Buc, France ({serge.muller,razvan.iordache}@ge.com).

Isabelle Bloch is with TELECOM ParisTech (ENST) - CNRS UMR 5141, 46, rue Barrault, 75013 Paris, France (isabelle.bloch@enst.fr).

Giovanni Palma is both with GE Healthcare and TELECOM ParisTech (giovanni.palma@ge.com).

This work was realized under CIFRE convention 20061165 (GE Healthcare/Telecom ParisTech).

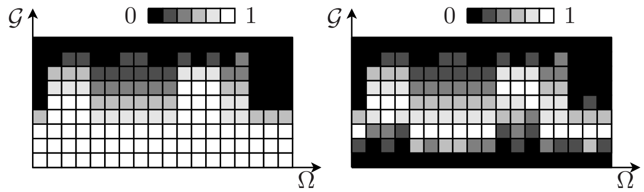

(a) (b)

Fig. 1. Example of Fuzzy Umbra Image (a) and Fuzzy Number Image (b) defined on a 1D space Ω.

in the images. Nonetheless, this can be highly application dependent. Moreover, it does not solve the issue of statistical noise. Actually, the definition of these images should be altered in order to be able to express it, for instance by using Fuzzy Random Variables [5]. Unfortunately, such a structure would be more complex to handle and hardly usable. This motivates a method to transform the noise component into some imprecision that fuzzy images could represent.

B. Fuzzy connected filters

Fuzzy images were originally introduced in order to express connected filters into the fuzzy set framework. The general expression of such filters relies on the definition of an (hyper-)connectivity defined on fuzzy sets of $\mathcal{S}$. Examples of fuzzy connectivity are proposed in [6], [7] and [8]. We denote $\mathcal{H}$ the set containing all the connected components of $\mathcal{S}$ according to the chosen definition of connectivity. Additionally, for a given fuzzy set $\nu \in \mathcal{S}$, $\mathcal{H}(\nu)$ denotes the set of the largest fuzzy connected components included in ν.

In the context of detection of structures, fuzzy connected filters are usually defined as follows:

$$\forall F \in \mathcal{F} \quad \xi(F) = \bigvee_{g \in \mathcal{G}} \bigvee \{\nu \in \mathcal{H}(F(.,g))/C(\nu) = 1\}$$

where C is a criterion equal to 1 if the fuzzy connected component is compatible with the searched structure and equal to 0 otherwise.

C. Fuzzy denoising based on the extension principle

In order to get rid of the noise in crisp images, denoising approaches exist. Unfortunately, they are usually parameter dependent, and do not provide exactly the original image without noise. Most of the time we get a trade-off, according to the choice of the tuned parameters, between noise removing and keeping information present in the image. Usually, the parameters are set once such that they optimize some criterion modeling this compromise. Of course different criteria would give different parameters with different properties. For instance we may want to be sure of keeping low contrasted structures at the expense of not removing all the noise, or on the contrary having a noise free image even if some structures are lost. In the case of detection, making a decision at this step may result in a loss of information and prevent the processing chain to give the right result. To avoid this problem, we could try to keep as much information as possible in order to make the decision later. Therefore, we can associate membership degrees to all possible parameter values in order to use the extension principle [9] leading to fuzzy gray levels. This would allow us to get a fuzzy image where the statistical noise component is transformed into denoising imprecision. In that case, the fuzzy image is completely suitable to represent it. This conversion step is a key idea that will be used throughout this paper.

Let us define such an approach in a generic way. Let I be the crisp image, Υ_γ a denosing filter and γ the parameter of the denoising method. If we are able to associate a membership degree μ_γ to each value of γ, we are able to associate a membership degree to each possible gray level at each pixel. The extension principle gives us:

$$\forall I : \Omega \to \mathcal{G}, \forall p \in \Omega, \forall g \in \mathcal{G} \quad F(p,g) = \sup_{\Upsilon_\gamma(I)(p)=g} \mu_\gamma$$

The problem of such an approach is the need for the computation of a large number of denoised images. For this reason, we develop in this paper the extension of a wavelet based denoising approach to the fuzzy set framework.

III. Fuzzy wavelet denoising

In this section we propose to detail the adaptation of a wavelet based denoising approach in order to generate a fuzzy image. First, we remind the principles of 1D wavelet decomposition and denoising. Then, we detail a method to model imprecision in this approach and show how to build a fuzzy image.

A. Wavelet decomposition

Wavelet analysis is a multi-resolution approach, which relies on the following definition:

Definition 3.1: A multi-resolution analysis is a sequence of nested, closed subspaces $\{V_j\} \subset L_2(\mathbb{R})$ verifying [10]:

$$\forall j \in \mathbb{Z} \quad V_j \subset V_{j+1}$$
$$\overline{\lim_{j\to\infty} V_j} = \overline{\bigcup_{j\in\mathbb{Z}} V_j} = L_2(\mathbb{R})$$
$$\lim_{j\to-\infty} \bigcap_{j\in\mathbb{Z}} V_j = \{0\}$$
$$f(x) \in V_j \Leftrightarrow f(2x) \in V_{j+1}, j \in \mathbb{Z} \text{ (scale invariance)}$$
$$f(x) \in V_0 \Leftrightarrow f(x+k) \in V_0, k \in \mathbb{Z} \text{ (shift invariance)}$$
$$\exists \phi(x) \in V_0 / \{\phi(x-k), k \in \mathbb{Z}\} \text{ is a stable basis for } V_0.$$

The first term means that for a given scale j, V_j is a subspace of V_{j+1}, resulting in a loss of information when projecting an element of V_{j+1} onto V_j. The second term means that with a large enough scale we can represent the original signal. The third term means that when j tends toward $-\infty$, all information about the signal is lost. Fourth and fifth terms imply that the same analysis can be done independently of scale and origin. Finally the last term is needed to deal with infinite dimensional vector spaces. The function $\phi(x)$ is called a father function or scaling function: basis functions of V_0 are then shifted versions of it. Stretching and normalizing it enables to produce basis functions for the various V_j.

As we said, for a given scale $j+1$, V_{j+1} enables to represent elements that V_j does not contain. For this reason we need to introduce the orthogonal complement W_j of V_j in V_{j+1}:

$$V_{j+1} = V_j \oplus W_j$$

More practically, each W_j will be generated using a basis composed of translations of a stretched mother function ψ, which is also denominated by wavelet function.

In order to analyze a given function at various scales, it is required to be able to express this function on the new basis. This can be achieved using a filter bank as proposed in [11]. This decomposition relies on four filters h, g, $\tilde{h}$ and $\tilde{g}$. These filters can be deduced from ϕ, ψ in the case of orthogonal wavelets and from their dual functions in the case of a bi-orthogonal wavelets. In both cases it allows us to reconstruct perfectly the original signal.

Let s_{j+1} be the approximation of the original signal f in V_{j+1}. This filter bank can be expressed mathematically using the following expressions:

$$s_{j,k} = \sum_{l \in \mathbb{Z}} \tilde{h}_{l-2k} s_{j+1,l}$$

where $s_{j,k}$ represents the coefficients of the approximation of s_{j+1} in V_j,

$$\omega_{j,k} = \sum_{l \in \mathbb{Z}} \tilde{g}_{l-2k} s_{j+1,l}$$

where $\omega_{j,k}$ represents the details of s_{j+1} expressed in W_j.

The reconstruction part can be expressed as:

$$s_{j+1,l} = \sum_{k \in \mathbb{Z}} h_{l-2k} s_{j,k} + \sum_{k \in \mathbb{Z}} g_{l-2k} \omega_{j,k} \quad (1)$$

The extension of this theoretical material in 2D is usually done by processing an image along the two orientations successively [10].

B. Wavelet shrinkage

Once the image is decomposed on the wavelet basis, the coefficients $\{\omega_{j,k}\}$ can be modified in order to make changes in the original image. Thanks to the properties of wavelet decomposition, several denoising approaches based on the suppression of small wavelet coefficients were proposed in the literature [10]. A first approach consists in a keep or kill strategy: large coefficients are kept while the others are set to zero. This approach is known as hard-thresholding. A second approach, which is more continuous, consists in subtracting, respectively adding, a given constant to positive coefficients, respectively negative ones, and to set to zero the ones whose sign has changed. This approach is known as soft-thresholding [12] and the transformation of a coefficient ω is mathematically defined for a threshold λ as:

$$\begin{cases} \max(0, \omega - \lambda) & \text{if } \omega \geq 0 \\ \min(0, \omega + \lambda) & \text{if } \omega < 0 \end{cases}$$

Both approaches rely on a threshold λ and produce more or less degraded/noisy images depending on this parameter. Optimization techniques exist to automatically set this threshold according to assumptions on the noise nature like the universal threshold technique [13], Stein's Unbiased Risk Estimation (SURE) [14] or the Generalized Cross Validation (GCV) approach [15]. The two last ones rely on the minimization of the mean square error between the denoised image and what would be the noise free image. In this paper, we will use the GCV approach, which assumes the image is corrupted with Gaussian noise, for soft-thresholding in order to derive our approach. Of course other techniques could be used as well.

C. Fuzzy coefficients

The thresholds obtained with these techniques usually correspond to a trade-off between the quantity of noise to be removed and the quantity of details to be kept after the processing. Our idea is that the choice we make at this stage could be weakened by the introduction of imprecision on this parameter. While crisp intervals are suitable to represent this imprecision, fuzziness enables to cope with common issues caused by the choice of crisp bounds. This motivates a fuzzification process of the wavelet coefficients ω_j.

Without a great loss of generality we can represent fuzzy numbers using an LR representation, which is a special case of LR fuzzy interval representation. Such fuzzy quantities are represented using two functions $L : \mathbb{R}^+ \to [0,1]$, $R : \mathbb{R}^+ \to [0,1]$ such that $L(0) = R(0) = 1$, $L(1) = R(1) = 0$ and $\forall x > 1$ $L(x) = R(x) = 0$. Additionally, four parameters (m_1, m_2, a, b) are required such that the membership function for a fuzzy interval $Q = (m_1, m_2, a, b)_{LR}$ is given by:

$$\begin{cases} \mu_Q(x) = L\left(\frac{m_1 - x}{a}\right) & \text{if } x \leq m_1 \\ \mu_Q(x) = 1 & \text{if } m_1 < x < m_2 \\ \mu_Q(x) = R\left(\frac{x - m_2}{b}\right) & \text{if } x \geq m_2 \end{cases}$$

In the case of a fuzzy number, the parameters m_1 and m_2 are equal. This representation is illustrated in Figure 2.

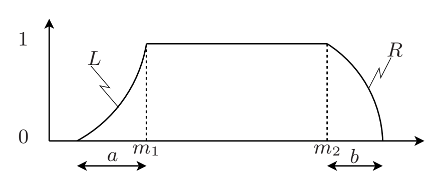

Fig. 2. LR representation of a fuzzy interval.

Back to the fuzzification of the wavelet coefficients, we propose an approach, in the case of soft-thresholding, based on the assumption that the most possible thresholded coefficient value is the one obtained with the GCV approach, and its worst value is obtained for the original coefficient value (i.e. $\lambda = 0$). This leads to the following fuzzification scheme:

$$\mu_\omega(x) = \begin{cases} (\max(\omega-\lambda,0), \max(\omega-\lambda,0), \\ \quad 0, \beta(\omega - \max(\omega-\lambda,0)))_{LR} \text{ if } \omega \geq 0 \\ (\min(\omega+\lambda,0), \min(\omega+\lambda,0), \\ \quad \beta(\min(\omega+\lambda,0)-\omega),0)_{LR} \text{ otherwise} \end{cases}$$

with β a parameter that allows us to tune the amount of imprecision we want to introduce. Figure 3 illustrates this fuzzification process. The core of the fuzzy coefficients, which appear in gray in the figure, is obtained from the optimal transfer function corresponding to the GCV method. The slope of these numbers is more or less steep according to the parameter β. When $\beta = 1$, the membership function is vanishing exactly at the original coefficient value.

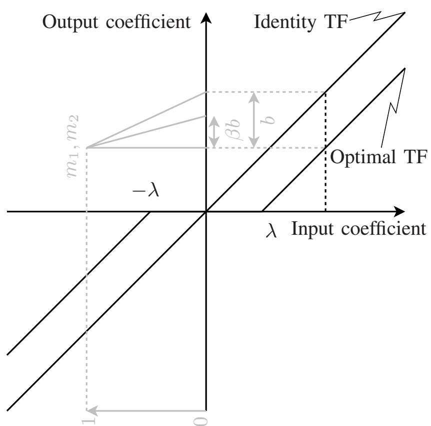

Fig. 3. Fuzzification process of a wavelet coefficient. A membership degree of 1 is associated to the coefficient value obtained for an optimal soft-thresholding. The membership value decreases when the new coefficient value gets closer to its original value. Identity TF and Optimal TF correspond to the transfer functions obtained for $\lambda = 0$ and for λ given by the GCV approach, respectively.

Because GCV is designed to suppress Gaussian noise, this fuzzification scheme allows it to be converted into some denoising imprecision on the wavelet coefficients. Let us remark this imprecision can be expressed using fuzzy number because semantics is not the same for this imprecision and for stochastic noise.

D. Generation of a fuzzy image

The main remaining problem is the reconstruction stage of the filter bank because the nature of some elements added and multiplied in Equation 1 changes: wavelet coefficients become fuzzy numbers. Nonetheless, the fuzzy set framework enables to define a fuzzy arithmetic on fuzzy numbers. Furthermore, using LR representations, common operators can easily be formulated. Thus if we consider two fuzzy intervals $Q_1 = (m, m', a, b)_{LR}$ and $Q_2 = (n, n', c, d)_{LR}$, we can express the fuzzy + operator as:

$$Q_1 \oplus Q_2 = (m+n, m'+n', a+c, b+d)_{LR} \quad (2)$$

The product operator between a fuzzy number and a positive crisp scalar is written:

$$\alpha \odot Q_1 = (\alpha m, \alpha m', \alpha a, \alpha b)_{LR}$$

while in the case of a negative scalar it is expressed as:

$$\alpha \odot Q_1 = (\alpha m', \alpha m, -\alpha b, -\alpha a)_{RL}$$

Because Equation 1 only needs these three definitions in the case of fuzzy coefficients $\{s_{j,k}\}$ and $\{\omega_{j,k}\}$, this expression can be rewritten as:

$$s_{j+1,l} = \sum_{k\in\mathbb{Z}}^{\oplus} h_{l-2k} \odot s_{j,k} + \sum_{k\in\mathbb{Z}}^{\oplus} g_{l-2k} \odot \omega j,k \quad (3)$$

with $\sum^{\oplus}$ the fuzzy counterpart of $\sum$ according to Equation 2.

Reconstructing completely a fuzzy image from this expression provides a fuzzy number image. Because the set of gray levels $\mathcal{G}$ is not continuous, sampling the fuzzy gray levels on this set may result in pixels where no gray levels have a membership degree equal to one. Clearly in that case we do not have a fuzzy number image. To overcome this limitation a last step consisting in dilating the continuous fuzzy gray levels can be done: we subtract, respectively add, $\frac{s}{2}$ to m_1, respectively m_2, with s the sampling step. This enables to ensure the core of the fuzzy gray level is large enough to have one gray level with a membership degree of 1 after the sampling. In the case we want a fuzzy umbra image, we can arbitrarily force the decreasingness with respect to the gray level from a fuzzy number image according to Definition 2.1.

E. Amount of fuzziness

As explained earlier, the parameter β introduced in the fuzzification process allows us to tune the amount of imprecision we introduce in the final fuzzy image. In order to quantify it, we need a measure like the fuzziness degree (fuzzy entropy) introduced in [16]. Because wavelet coefficients are real numbers in our context we use a continuous version of the measure:

$$G(\mu) = -\int_{-\infty}^{\infty} \begin{array}{l} \mu(x)\log_2(\mu(x)) \\ \quad +(1-\mu(x))\log_2(1-\mu(x))dx \end{array}$$

Theorem 3.1: $\forall \beta \in \mathbb{R}^+$, for fuzzy intervals $Q^\beta = (m_1, m_2, \beta a, \beta b)_{LR}$, we have $G(\mu_{Q^\beta}) = \beta G(\mu_{Q^1})$.

Proof: By definition, we have:

$$\begin{aligned} G(\mu_{Q^\beta}) = & -\int_{-\infty}^{m_1} R(\tfrac{m_1-x}{\beta a})\log_2 R(\tfrac{m_1-x}{\beta a})dx \\ & -\int_{m_1}^{m_2} 1\log(1)dx \\ & -\int_{m_2}^{\infty} L(\tfrac{x-m_2}{\beta b})\log_2 L(\tfrac{x-m_2}{\beta b})dx \\ & -\int_{-\infty}^{m_1}(1-R(\tfrac{m_1-x}{\beta a}))\log_2(1-R(\tfrac{m_1-x}{\beta a}))dx \\ & -\int_{m_1}^{m_2} 0\log(0)dx \\ & -\int_{m_2}^{\infty}(1-R(\tfrac{x-m_2}{\beta b}))\log_2(1-R(\tfrac{x-m_2}{\beta b}))dx \end{aligned}$$

the second and fifth terms are null, and the other terms are stretched versions of the integration of R and L on $[0, 1]$, which leads to:

$$\begin{aligned} G(\mu_{Q^\beta}) = & -\beta a \int_0^1 R(x)\log_2(R(x))dx \\ & -\beta b \int_0^1 L(x)\log_2(L(x))dx \\ & -\beta a \int_0^1 (1-R(x))\log_2(1-R(x))dx \\ & -\beta b \int_0^1 (1-L(x))\log_2(1-L(x))dx \end{aligned}$$

Thus we have $G(\mu_{Q^\beta}) = \beta G(\mu_{Q^1})$. ■

Let us define the degree of fuzziness of a fuzzy image, or fuzziness amount per pixel (*fapp*):

Definition 3.2: Let F be a fuzzy image:

$$fapp(F) = \frac{1}{|\Omega|} \sum_{p \in \Omega} G(F(p,.))$$

We can finally introduce a last theorem:

Theorem 3.2: Let I be a crisp image, $\beta \in \mathbb{R}^+$ and F^β be the fuzzified version of I using parameter β, we have:

$$fapp(F^\beta) = \beta fapp(F^1)$$

Proof: Let I be a crisp image. Using Equation 3 and the definitions of $\oplus$ and $\odot$, there exist $\{Q_i^\gamma = (m_1^i, m_2^i, \gamma a^i, \gamma b^i)\}$ defined for $\gamma \in \mathbb{R}^+$ such that $\forall \beta \in \mathbb{R}^+$ the fuzzified image F^β verifies: $\forall p_i \in \Omega$ $F^\beta(p_i,.) = Q_i^\beta$. Thus using Theorem 3.1, we can deduce that $G(F^\beta(p_i,.)) = G(Q_i^\beta) = \beta G(Q_i^1) = \beta G(F^1(p_i,.))$.

Finally, using Definition 3.2 we can conclude that Theorem 3.2 is verified. ■

This theorem is useful because if we want to construct several images $\{F^\beta\}$ that have given *fapp* values, we only need to produce one fuzzy image F^1, and then deduce the set of β needed. Furthermore, for any β, F^β can directly be computed from F^1 because β is multiplying parameters a^i and b^i of the fuzzy numbers in the reconstructed fuzzy image.

IV. Results

In order to assess the robustness of the method, it was tested on synthetic images degraded with Gaussian noise or Poisson noise. The original image is composed of twenty five disks lying on a constant background as shown in Figure 4. The gray levels of the disks from top left to bottom right are decreasing starting from the intensity of the background minus one. This leads to disks with an increasing contrast to noise ratio. Without noise, this image allows us to extract all the disks using a strict definition of flat zones in addition to a criterion on the size of the disks. In this experiment, the capability to extract the same zones in presence of noise using a FNI and the definition of fuzzy flat zones is evaluated.

A. Experiments

In each case, the degraded image is decomposed on a Daubechies wavelets basis [17] using four scales. Then the wavelet coefficients are fuzzified in order to generate a fuzzy number image using the method described in the previous section. In order to extract the disks, the fuzzy image is then processed by the following connected filter:

$$\forall F \in \mathcal{F}\ \xi(F) = \bigvee_{g \in \mathcal{G}} \bigvee \{\nu \in \mathcal{H}(\nu) / (a_1 < A(\nu) < a_2)\} \quad (4)$$

with A a fuzzy area measure, a_1 and a_2 two constants that enclose the area of disks in the original image.

This filter can be seen as producing a fuzzy set resulting from the aggregation of the detected fuzzy connected components corresponding to the different disks. An example of this detection in the image of Figure 4(b) is given in

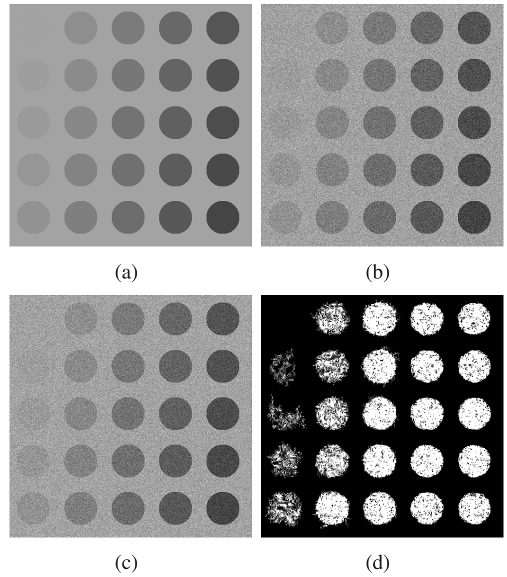

Fig. 4. (a) Original image composed of 25 synthetic disks of different contrast values. (b) The same image with Gaussian noise (standard deviation equal to 16.5). (c) The same image with Poisson noise. (d) Result of the detection in the image (b) for a *fapp* equal to 5.

Figure 4(d). Ideally, this set is equal to one within the disks and equal to 0 in the background. Thus for each disk we compute a similarity measure [18] with the crisp set equal to one in the considered disk and equal to 0 elsewhere in order to evaluate the quality of the detection. Doing this for each disk enables to assess how the method behaves for different CNR values. Obviously, the fuzziness amount in the image plays an important role in the ability to detect structures. Using Theorem 3.2, the former similarities of detected disks can easily be evaluated for various *fapp* values without reconstructing a fuzzy image at each time.

B. Gaussian noise

Figure 5 illustrates the detection capability of the approach for the image of Figure 4(b), which contains Gaussian noise. We observe that for any CNR value, there is an optimal fuzziness amount per pixel value for the detection of the corresponding disk. Too small values of *fapp* do not allow reconnecting disks while too large values tend to merge the disk in the background resulting in a non detection. A second key point is that the optimal values of *fapp* depend on the contrast to noise ratio of the disk. Thus there is no way to fuzzify an image such that all structures of different contrast can be extracted optimally. The optimal *fapp* values are closer to 0 for lower CNR values than for higher ones. Nonetheless, in the case of detection, compromises can be found. Indeed, if we choose a *fapp* optimizing the detection of a contrasted enough structure, the detection of higher contrast structures can be good enough: in most applications, an imperfect mask of the structure is suitable for further processing such as segmentation.

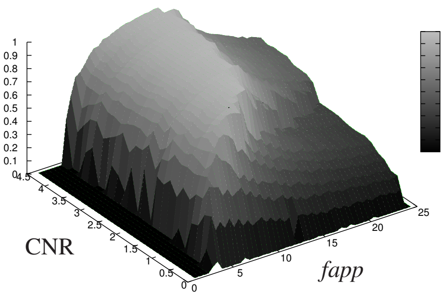

Fig. 5. Evolution of the similarity between the disks present in the image of Figure 4(a) and their detection using Equation 4 in the image corrupted with Gaussian noise of Figure 4(b). The similarities are given according to their CNR and the amount of fuzziness (*fapp*) introduced in the fuzzy image.

C. Poisson Noise

In the case of an image containing Poisson noise, the wavelet denoising approach we propose in this paper cannot be directly applied because the GCV method proposed in [10] assumes that the input image in corrupted with Gaussian noise. Nonetheless, as proposed in [19] we can pre-process the crisp image with a transfer function in order to get data with a distribution closer to the Gaussian.

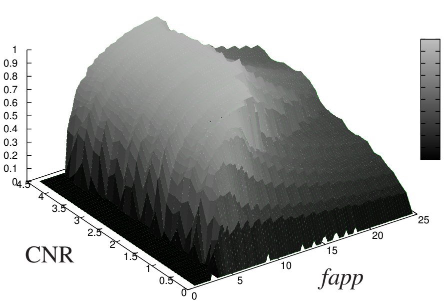

Fig. 6. Evolution of the similarity between the disks present in the image of Figure 4(a) and their detection using Equation 4 in the image corrupted with Poisson noise of Figure 4(c). The similarities are given according to their CNR and the amount of fuzziness (*fapp*) introduced in the fuzzy image.

The evolution of the detectability for this noise configuration is different from the Gaussian case as illustrated in Figure 6. Here, low *fapp* values allow to retrieve high contrasted disks first. This result is coherent with the fact that in the proposed synthetic image, the background has a higher intensity compared to the disks, therefore disks are demonstrating less noise. Actually, due to the nature of the noise, when the contrast increases the noise in the disks decreases, making their detection requiring less fuzziness. Finally, conclusions drawn in the Gaussian case about *fapp* optimal values and their dependence on the contrast are still valid.

V. Conclusion

In this paper we addressed the problem of fuzzy image construction. Our approach is generic and relies on the conversion of statistical noise present in the input image into an imprecision on gray levels that can be obtained with a denoising approach. We focused on the description of a wavelet decomposition and showed how to fuzzify the wavelet coefficients in order to produce a fuzzy number image.

We also discussed the impact of fuzzification on the detectability of structures in a synthetic image. We showed that for Gaussian and Poisson noises, the optimal amount of fuzziness to be introduced in the image depends on the contrast to noise ratio of the target structure.

References

[1] P. Salembier and J. Serra, "Flat zones filtering, connected operators, and filters by reconstruction," *IEEE Transactions on Image Processing*, vol. 4, no. 8, pp. 1153–1160, 1995.
[2] E. Breen and R. Jones, "Attribute Openings, Thinnings, and Granulometries," *Computer Vision and Image Understanding*, vol. 64, no. 3, pp. 377–389, 1996.
[3] G. Palma, I. Bloch, and S. Muller, "Fuzzy Connected Filters for Fuzzy Gray Scale Images," in *IPMU'08*, Malaga, Spain, jun 2008, pp. 667–674.
[4] G. Palma, O. Nempont, I. Bloch, and S. Muller, "Extraction de "zones plates floues" dans des images de quantités floues," in *Rencontre Francophones sur la Logique Floue et ses Applications*, Lens, France, oct 2008.
[5] M. Lopez-Diaz and M. A. Gil, "Constructive definitions of fuzzy random variables," *Statistics & Probability Letters*, vol. 36, no. 2, pp. 135–143, December 1997.
[6] A. Rosenfeld, "Fuzzy Digital Topology," *Information and Control*, vol. 40, pp. 76–87, 1979.
[7] U. Braga-Neto and J. Goutsias, "A Theoretical Tour of Connectivity in Image Processing and Analysis," *Journal of Mathematical Imaging and Vision*, vol. 19, no. 1, pp. 5–31, 2003.
[8] O. Nempont, J. Atif, E. Angelini, and I. Bloch, "A New Fuzzy Connectivity Class. Application to Structural Recognition in Images," in *DGCI*, Lyon, 2008, pp. 446–557.
[9] L. A. Zadeh, "The concept of a linguistic variable and its application to approximate reasoning-III," *Information Sciences*, vol. 9, no. 1, pp. 43–80, 1975.
[10] M. Jansen, *Noise Reduction by Wavelet Thresholding*. Springer, 2001.
[11] S. G. Mallat, "A Theory for Multiresolution Signal Decomposition: The Wavelet Representation," *IEEE Transactions on Pattern Analysis and Machine Intelligence*, vol. 11, no. 7, July 1989.
[12] D. L. Donoho, "De-noising by soft-thresholding," *IEEE Transactions on Information Theory*, vol. 41, no. 3, pp. 613–627, 1995.
[13] D. L. Donoho, I. M. Johnstone, G. Kerkyacharian, and D. Picard, "Wavelet shrinkage: asymptopia? (with discussion)," *Journal of the Royal Statistical Society: Series B (Statistical Methodology)*, vol. 57, pp. 301–369, 1995.
[14] D. L. Donoho and I. M. Johnstone, "Adapting to unknown smoothness via wavelet shrinkage," *Journal of the American Statistical Association*, vol. 90, no. 432, pp. 1200–1224, 1995.
[15] M. Jansen, M. Malfait, and A. Bultheel, "Generalized cross validation for wavelet thresholding," *Signal Processing*, vol. 56, pp. 33–44, 1997.
[16] A. De Luca and S. Termini, "A definition of Non-Probabilistic Entropy in the Setting of Fuzzy Sets Theory," *Information Control*, vol. 20, pp. 301–312, 1972.
[17] I. Daubechies, "Orthonormal bases of compactly supported wavelets," *J. Comm. Pure appl. Math.*, vol. 41, pp. 909–996, Oct. 1988.
[18] M. Rifqi, "Mesures de comparaison, typicalité et classification d'objets flous: théorie et pratique," Ph.D. dissertation, LAFORIA TH96/15, Institut Blaise Pascal, 1996.
[19] F. J. Anscombe, "The Transformation of Poisson, Binomial And Negative-Binomial Data," *Biometrika*, vol. 35, no. 3-4, pp. 246–254, 1948.